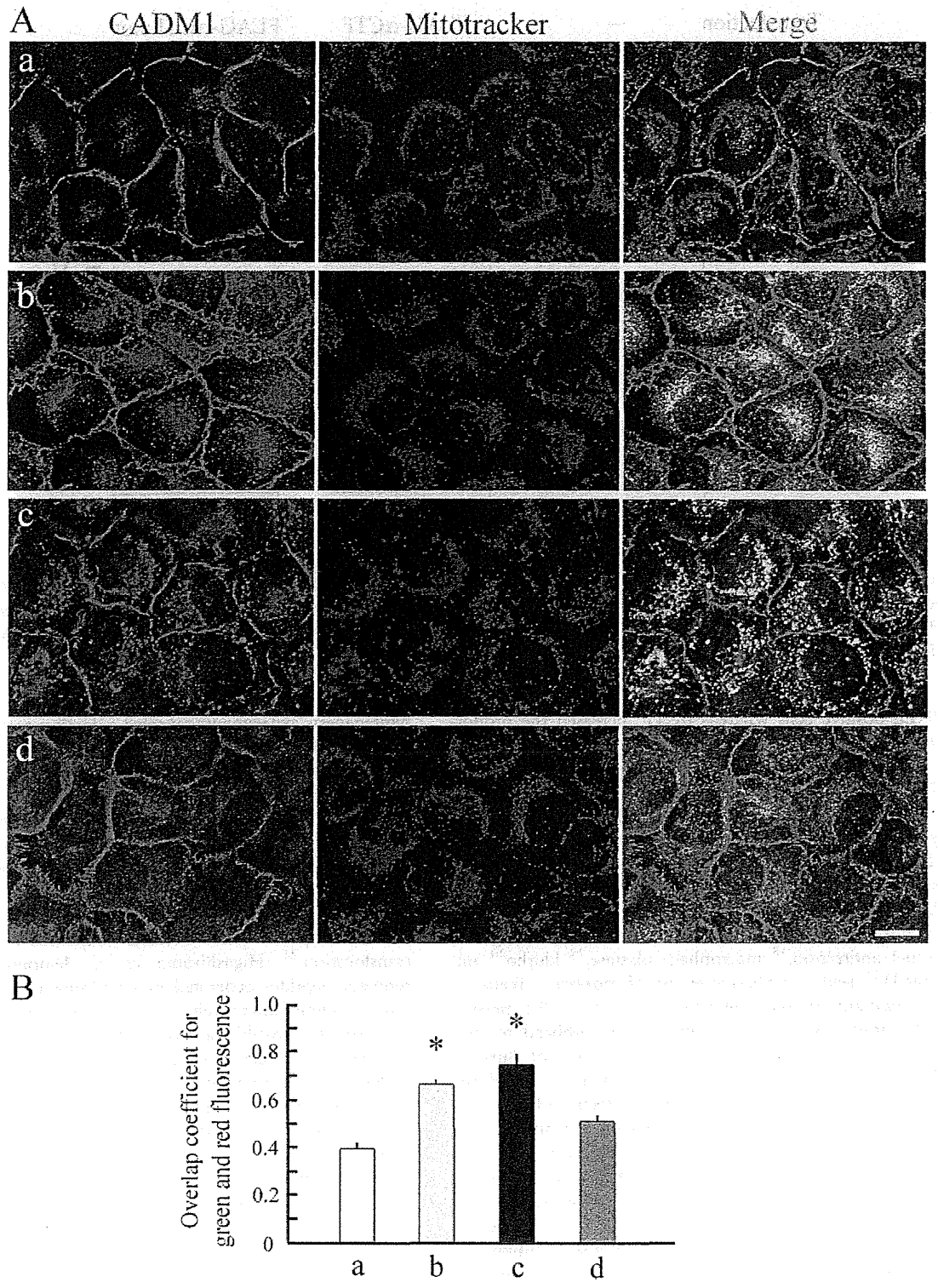

Figure 4 Immunofluorescence of cell adhesion molecule 1 (CADM1) with Mitotracker staining in NCI-H441 cells expressing α C terminal fragment (CTF) and αCTFmut. (A) NCI-H441 cells were untreated (a) or treated with a mixture of phorbol myristic acid and trypsin (b), or were transfected with pCX4bsr-SP-αCTF (c) or pCX4bsr-SP-αCTFmut (d). Then, cells were double stained with CADM1 immunofluorescence (green; left) and Mitotracker fluorescence (red; middle). In the merged images (right), yellow areas mean colocalisation of both fluorescent signals—that is, mitochondrial localisation of CADM1. Bar=10 μm. (B) Graph showing overlap coefficients in NCI-H441 cells of the four types (a–d shown in (A)). Intensity correlation between green and red fluorescence was quantified using ImageJ Colocalisation Analysis, and overlap coefficients were calculated. Data are expressed as mean±SD, and statistical significance was analysed by the Student's t test. *p<0.01 compared with the value of untreated cells (a in (A)).

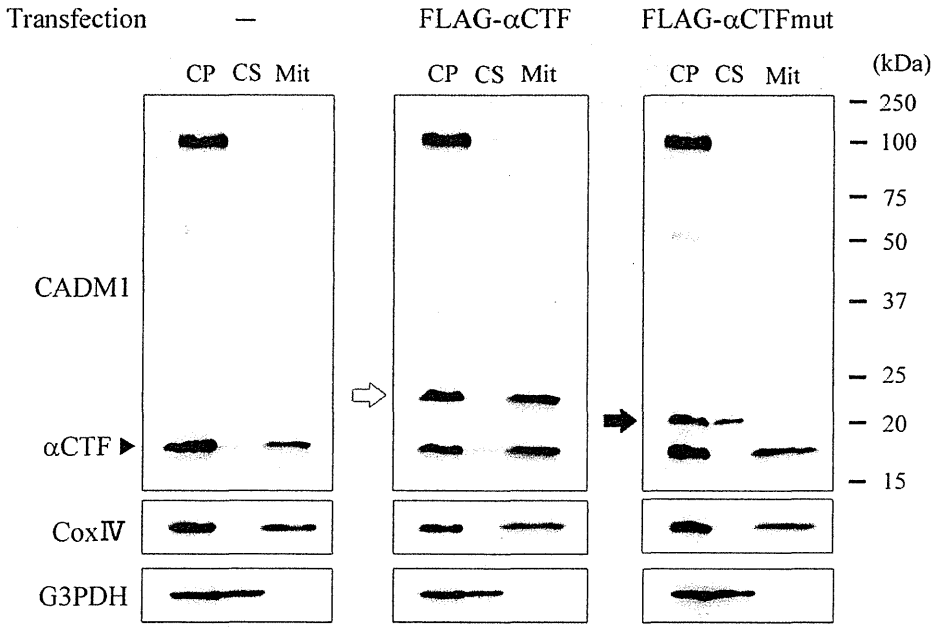

Figure 5 Cell fractionation experiments of NCI-H441 cells expressing α C terminal fragment (CTF) and αCTFmut. NCI-H441 cells were untransfected (left) or transfected with p3xFLAG-αCTF (middle) or p3xFLAG-αCTFmut (right), and were fractionated into cytosolic (CS) and mitochondrial (Mit) fractions. Whole cytoplasmic lysates (CP) were extracted from aliquots of the cells. These lysates and fractions were analysed with western blotting using antibodies against cell adhesion molecule 1 (CADM1), cytochrome c oxidase subunit IV (CoxIV) and glyceraldehyde 3-phosphate dehydrogenase (G3PDH). Open and closed arrows indicate FLAG tagged αCTF and αCTFmut, respectively.

of TUNEL positive cells whereas αCTF increased the proportion fivefold ($p<0.01$) (figure 6B).

DISCUSSION

We found that CADM1 ectodomain shedding increased in emphysematous lungs from smoking patients, but not in normal lungs from smoking patients, suggesting that oxidants in cigarette smoke may act as a critical inducer of CADM1 ectodomain shedding only in subjects who have particular genetic backgrounds. Of interest, changes in emphysema susceptible genes, such as α-1 antitrypsin,[18] macrophage elastase,[19] klotho[20] and surfactant D,[21] lead to a relative excess of proteases, creating a local protease/antiprotease imbalance.[19 21–23] In the present study, all patients with smoking habits were obliged to quit smoking more than 1 month before the date of surgery. Therefore, oxidants seem not to promote CADM1 shedding through its direct ongoing action but rather seem to help establish long lasting protease/antiprotease imbalances in alveoli.

All but one patient (case No 19) analysed in this study had lung cancer. Because CADM1 is known to be downregulated in lung cancer due to promoter methylation,[24] these patients had potentially impaired CADM1 expression even in non-cancerous lungs. We performed western blot analyses of a small number of emphysematous lungs that did not develop lung cancer, and detected a relative increase in αCTF and βCTF to full length CADM1 (see online supplementary figure S7). Increased amounts of αCTF and βCTF appeared to be present in emphysematous lungs as a result of increased ectodomain shedding of CADM1 in emphysematous lungs, both with and without lung cancer.

Cell fractionation and immunofluorescence experiments consistently showed that αCTF localised to mitochondria. This finding appeared to be relevant in vivo, as we detected intracytoplasmic CADM1 that was associated with mitochondria in alveolar epithelial cells from emphysematous lungs (figure 2D). Mutagenesis experiments revealed a decisive role for the intracytoplasmic domain in this subcellular localisation. How the intracytoplasmic domain leads αCTF to mitochondria remains to be addressed. A growing body of evidence is accumulating to show that cell membrane spanning proteins, such as epidermal growth factor receptor and mucin 1, can translocate to mitochondria.[25 26] Although mechanisms underlying these events remain largely unknown, clathrin mediated endocytosis is shown to be involved.[26] After internalisation, mucin 1 is assumed to utilise heat shock proteins as molecular chaperons for mitochondrial translocation.[25] Higashiyama *et al* demonstrated that the remnant peptides generated by ectodomain shedding of type I integral membrane proteins, such as pro-heparin binding epidermal growth factor-like growth factor and pro-amphiregulin, are internalised into endocytotic vesicles.[27 28] The N and C termini of the peptides are positioned inside and outside of the vesicles, respectively, and the C terminal tail, free in the cytosol, plays a decisive role in the intracellular destinations of the remnant peptide.[27 28] αCTF may be present as a vesicle associated transmembrane molecule in the cytoplasm, with its C terminal tail being free outside the vesicle, and this C terminal tail may carry a conformational signal that serves as a binding site for molecular chaperons, such as heat shock protein family members.

Exogenous αCTF decreased mitochondrial membrane potential in NCI-H441 cells and increased apoptosis, suggesting that mitochondrial localisation of αCTF might result in activation of the mitochondrial apoptosis pathway. Mao *et al* reported that exogenous CADM1 induces caspase 3 activation and apoptosis in A549 lung adenocarcinoma cells lacking endogenous CADM1, and that protein 4.1 binding motif and PDZ domain binding motif in the intracytoplasmic domain are indispensable for this induction.[29] Members of the membrane associated guanylate kinase (MAGuK) family are known as binding partners to the latter motif.[30] Interestingly, this family contains a subgroup that carries the caspase recruitment domain in its N terminal

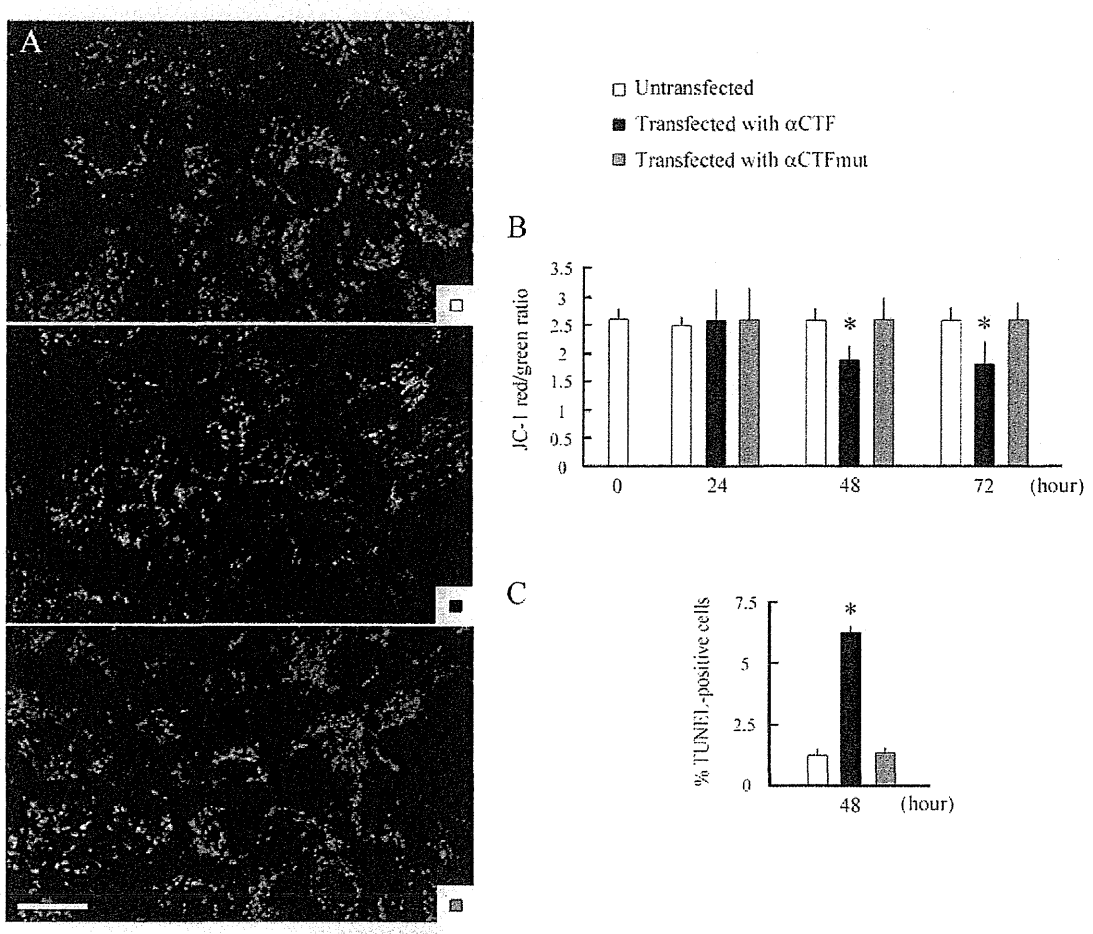

Figure 6 α C terminal fragment (CTF) decreases mitochondrial membrane potential in NCI-H441 cells and increases apoptosis. (A) Representative results of JC-1 staining in NCI-H441 cells. NCI-H441 cells were untransfected (upper) or transfected with pCX4bsr-SP-αCTF (middle) or pCX4bsr-SP-αCTFmut (lower), and were stained 48 h later with JC-1 dye. Images were captured by a confocal laser microscope, and green and red fluorescence signals were merged. Differential interference contrast images are shown in online supplementary figure S6. Bar=20 μm. (B) Graph showing changes in JC-1 red/green ratios in NCI-H441 cells after transfection. NCI-H441 cells were untransfected or transfected with pCX4bsr-SP-αCTF or pCX4bsr-SP-αCTFmut, and were stained with JC-1 dye at the indicated time points. Cells were observed through a confocal laser microscope and were morphometrically analysed to calculate JC-1 red/green ratios. Data are expressed as mean± SD, and statistical significance was analysed by the Student's t test. *p<0.01 compared with the value of untransfected cells. (C) Graph showing the proportion of terminal deoxynucleotidyl transferase dUTP nick end labelling (TUNEL) positive NCI-H441 cells at 2 days after transfection. Cells were transfected as in (B). After 2 days, cells were stained with the TUNEL method, and the proportions of TUNEL positive cells were calculated. Data are expressed as mean±SD, and statistical significance was analysed by the Mann–Whitney U test. *p<0.01 compared with the value in untransfected cells.

region and participates in apoptosis signalling.[31] αCTF and βCTF, which both share the intracytoplasmic domain, once produced, may activate the mitochondrial apoptosis pathway by transporting particular MAGuK family members to mitochondria in alveolar epithelial cells.

There are several splice variants of human CADM1, named isoforms SP1 to SP4.[32] Reverse transcription-PCR revealed that nine lungs examined and NCI-H441 cells all expressed SP4 exclusively (see online supplementary figure S8). Tanabe *et al* showed that SP1 and SP2 are shed constitutively, while SP3 is non-cleavable.[33] Our data proved SP4 cleavable. SP4 ectodomain shedding appeared to be not constitutive but induced by particular pathological stimuli. Moiseeva *et al* reported that SP4 overexpressing HMC-1 mast cells show better survival and lower caspase 3/7 activity than SP1 overexpressing cells.[34] This difference between two isoforms may be explained by their distinct susceptibility to ectodomain shedding. In HMC-1 cells, SP1 may produce more αCTF and/or βCTF than SP4, resulting in activation of the mitochondrial apoptosis pathway.

In conclusion, we propose increased ectodomain shedding of CADM1 as a novel molecular mechanism for increased alveolar cell apoptosis in emphysematous lungs. This mechanism is an extension of the conventional understanding that proteolytic activity is locally excessive in emphysematous lung alveoli because CADM1 ectodomain shedding per se is a proteolytic process, and also suggests that selective inhibitors to block CADM1 sheddase activity and/or mitochondrial localisation of CADM1 shedding products can slow or halt the progression of emphysema. In fact, ADAM10 is released by human alveolar macrophages, and intratracheal administration of an adenoviral vector expressing ADAM10 in mice results in the development of emphysema.[35] Further characterisation of CADM1 ectodomain shedding and its associated molecular events will open a new avenue for target based therapeutic approaches to emphysema.

Contributors AI and YM designed the study, and AI wrote the manuscript. AI, TM and MO provided the clinical samples. TM, MH, TI, AY and TK performed the experiments, and MH analysed the data.

Funding This study was supported by the Japan Society for the Promotion of Science Kakenhi (24890274 and 25860302 to MH, 24659184 to TI, 24890137 to TM, and 24590492 to AI), and grants from the Yasuda Medical Foundation and the Osaka Medical Research Foundation for Intractable Diseases.

Competing interests None.

Patient consent Obtained.

Ethics approval Ethics approval was provided by the ethics committee of Hiroshima University and Kinki University, Japan (approval Nos Eki-350 and 25–088).

Provenance and peer review Not commissioned; externally peer reviewed.

REFERENCES

1 Snider GL, Kleinerman J, Thurlbeck WM, *et al*. The definition of emphysema. Report of a National Heart, Lung, and Blood Institute, Division of Lung Diseases workshop. *Am Rev Respir Dis* 1985;132:182–85.
2 Tuder RM, Petrache I, Elias JA, *et al*. Apoptosis and emphysema: the missing link. *Am J Respir Cell Mol Biol* 2003;28:551–4.
3 Taraseviciene-Stewart L, Voelkel NF. Molecular pathogenesis of emphysema. *J Clin Invest* 2008;118:394–402.
4 Demedts IK, Demoor T, Bracke KR, *et al*. Role of apoptosis in the pathogenesis of COPD and pulmonary emphysema. *Respir Res* 2006;7:53.
5 Suzuki T, Yamashita C, Zemans RL, *et al*. Leukocyte elastase induces lung epithelial apoptosis via a PAR-1-, NF-kappaB-, and p53-dependent pathway. *Am J Respir Cell Mol Biol* 2009;41:742–55.
6 Zheng T, Kang MJ, Crothers K, *et al*. Role of cathepsin S-dependent epithelial cell apoptosis in IFN-gamma-induced alveolar remodeling and pulmonary emphysema. *J Immunol* 2005;174:8106–15.
7 Powell WC, Fingleton B, Wilson CL, *et al*. The metalloproteinase matrilysin proteolytically generates active soluble Fas ligand and potentiates epithelial cell apoptosis. *Curr Biol* 1999;9:1441–7.
8 Mohan MJ, Seaton T, Mitchell J, *et al*. The tumor necrosis factor-alpha converting enzyme (TACE): a unique metalloproteinase with highly defined substrate selectivity. *Biochemistry* 2002;41:9462–9.
9 Kuramochi M, Fukuhara H, Nobukuni T, *et al*. TSLC1 is a tumor-suppressor gene in human non-small-cell lung cancer. *Nat Genet* 2001;27:427–30.
10 Ito A, Okada M, Uchino K, *et al*. Expression of the TSLC1 adhesion molecule in pulmonary epithelium and its down-regulation in pulmonary adenocarcinoma other than bronchioloalveolar carcinoma. *Lab Invest* 2003;83:1175–83.
11 Ito A, Nishikawa Y, Ohnuma K, *et al*. SgIGSF is a novel biliary-epithelial cell adhesion molecule mediating duct/ductule development. *Hepatology* 2007;45:684–94.
12 Sakurai-Yageta M, Masuda M, Tsuboi Y, *et al*. Tumor suppressor CADM1 is involved in epithelial cell structure. *Biochem Biophys Res Commun* 2009;390:977–82.
13 Fogel AI, Li Y, Giza J, *et al*. N-glycosylation at the SynCAM (synaptic cell adhesion molecule) immunoglobulin interface modulates synaptic adhesion. *J Biol Chem* 2010;285:34864–74.
14 Nagara Y, Hagiyama M, Hatano N, *et al*. Tumor suppressor cell adhesion molecule 1 (CADM1) is cleaved by a disintegrin and metalloprotease 10 (ADAM10) and subsequently cleaved by gamma-secretase complex. *Biochem Biophys Res Commun* 2012;417:462–7.
15 Kikuchi S, Yamada D, Fukami T, *et al*. Hypermethylation of the TSLC1/IGSF4 promoter is associated with tobacco smoking and a poor prognosis in primary nonsmall cell lung carcinoma. *Cancer* 2006;106:1751–8.
16 Ding K, Lopez-Burks M, Sanchez-Duran JA, *et al*. Growth factor-induced shedding of syndecan-1 confers glypican-1 dependence on mitogenic responses of cancer cells. *J Cell Biol* 2005;171:729–38.
17 Chyung AS, Greenberg BD, Cook DG, *et al*. Novel beta-secretase cleavage of beta-amyloid precursor protein in the endoplasmic reticulum/intermediate compartment of NT2N cells. *J Cell Biol* 1997;138:671–80.
18 Martorana PA, Brand T, Gardi C, *et al*. The pallid mouse. A model of genetic alpha 1-antitrypsin deficiency. *Lab Invest* 1993;68:233–41.
19 Hautamaki RD, Kobayashi DK, Senior RM, *et al*. Requirement for macrophage elastase for cigarette smoke-induced emphysema in mice. *Science* 1997;277:2002–4.
20 Kuro-o M, Matsumura Y, Aizawa H, *et al*. Mutation of the mouse klotho gene leads to a syndrome resembling ageing. *Nature* 1997;390:45–51.
21 Wert SE, Yoshida M, LeVine AM, *et al*. Increased metalloproteinase activity, oxidant production, and emphysema in surfactant protein D gene-inactivated mice. *Proc Natl Acad Sci U S A* 2000;97:5972–7.
22 Kidokoro Y, Kravis TC, Moser KM, *et al*. Relationship of leukocyte elastase concentration to severity of emphysema in homozygous alpha1-antitrypsin-deficient persons. *Am Rev Respir Dis* 1977;115:793–803.
23 Funada Y, Nishimura Y, Yokoyama M. Imbalance of matrix metalloproteinase-9 and tissue inhibitor of matrix metalloproteinase-1 is associated with pulmonary emphysema in Klotho mice. *Kobe J Med Sci* 2004;50:59–67.
24 Fukami T, Fukuhara H, Kuramochi M, *et al*. Promoter methylation of the TSLC1 gene in advanced lung tumors and various cancer cell lines. *Int J Cancer* 2003;107:53–9.
25 Ren J, Bharti A, Raina D, *et al*. MUC1 oncoprotein is targeted to mitochondria by heregulin-induced activation of c-Src and the molecular chaperone HSP90. *Oncogene* 2006;25:20–31.
26 Demory ML, Boerner JL, Davidson R, *et al*. Epidermal growth factor receptor translocation to the mitochondria: regulation and effect. *J Biol Chem* 2009;284:36592–604.
27 Hieda M, Isokane M, Koizumi M, *et al*. Membrane-anchored growth factor, HB-EGF, on the cell surface targeted to the inner nuclear membrane. *J Cell Biol* 2008;180:763–9.
28 Isokane M, Hieda M, Hirakawa S, *et al*. Plasma-membrane-anchored growth factor pro-amphiregulin binds A-type lamin and regulates global transcription. *J Cell Sci* 2008;121:3608–18.
29 Mao X, Seidlitz E, Truant R, *et al*. Re-expression of TSLC1 in a non-small-cell lung cancer cell line induces apoptosis and inhibits tumor growth. *Oncogene* 2004;23:5632–42.
30 Murakami Y. Involvement of a cell adhesion molecule, TSLC1/IGSF4, in human oncogenesis. *Cancer Sci* 2005;96:543–52.
31 Bertin J, Wang L, Guo Y, *et al*. CARD11 and CARD14 are novel caspase recruitment domain (CARD)/membrane-associated guanylate kinase (MAGUK) family members that interact with BCL10 and activate NF-kappa B. *J Biol Chem* 2001;276:11877–82.
32 Biederer T. Bioinformatic characterization of the SynCAM family of immunoglobulin-like domain-containing adhesion molecules. *Genomics* 2006;87:139–50.
33 Tanabe Y, Kasahara T, Momoi T, *et al*. Neuronal RA175/SynCAM1 isoforms are processed by tumor necrosis factor-alpha-converting enzyme (TACE)/ADAM17-like proteases. *Neurosci Lett* 2008;444:16–21.
34 Moiseeva EP, Leyland ML, Bradding P. CADM1 is expressed as multiple alternatively spliced functional and dysfunctional isoforms in human mast cells. *Cell Mol Life Sci* 2012;69:2751–64.
35 Saitoh H, Leopold PL, Harvey BG, *et al*. Emphysema mediated by lung overexpression of ADAM10. *Clin Transl Sci* 2009;2:50–6.

THORAX

Increased ectodomain shedding of lung epithelial cell adhesion molecule 1 as a cause of increased alveolar cell apoptosis in emphysema

Takahiro Mimae, Man Hagiyama, Takao Inoue, et al.

Thorax 2014 69: 223-231 originally published online October 2, 2013
doi: 10.1136/thoraxjnl-2013-203867

CHEST

Original Research

LUNG CANCER

Appropriate Sublobar Resection Choice for Ground Glass Opacity-Dominant Clinical Stage IA Lung Adenocarcinoma

Wedge Resection or Segmentectomy

Yasuhiro Tsutani, MD, PhD; Yoshihiro Miyata, MD, PhD; Haruhiko Nakayama, MD, PhD; Sakae Okumura, MD, PhD; Shuji Adachi, MD, PhD; Masahiro Yoshimura, MD, PhD; and Morihito Okada, MD, PhD

Background: **The purpose of this multicenter study was to characterize ground glass opacity (GGO)-dominant clinical stage IA lung adenocarcinomas and evaluate prognosis of these tumors after sublobar resection, such as segmentectomy and wedge resection.**

Methods: **We evaluated 610 consecutive patients with clinical stage IA lung adenocarcinoma who underwent complete resection after preoperative high-resolution CT scanning and ^{18}F-fluorodeoxyglucose PET/CT scanning and revealed 239 (39.2%) that had a >50% GGO component.**

Results: **GGO-dominant tumors rarely exhibited pathologic invasiveness, including lymphatic, vascular, or pleural invasion and lymph node metastasis. There was no significant difference in 3-year recurrence-free survival (RFS) among patients who underwent lobectomy (96.4%), segmentectomy (96.1%), and wedge resection (98.7%) of GGO-dominant tumors ($P = .44$). Furthermore, for GGO-dominant T1b tumors, 3-year RFS was similar in patients who underwent lobectomy (93.7%), segmentectomy (92.9%), and wedge resection (100%, $P = .66$). Two of 84 patients (2.4%) with GGO-dominant T1b tumors had lymph node metastasis. Multivariate Cox analysis showed that tumor size, maximum standardized uptake value on ^{18}F-fluorodeoxyglucose PET/CT scan, and surgical procedure did not affect RFS in GGO-dominant tumors.**

Conclusions: **GGO-dominant clinical stage IA lung adenocarcinomas are a uniform group of tumors that exhibit low-grade malignancy and have an extremely favorable prognosis. Patients with GGO-dominant clinical stage IA adenocarcinomas can be successfully treated with wedge resection of a T1a tumor and segmentectomy of a T1b tumor.** ***CHEST 2014; 145(1):66–71***

Abbreviations: FDG = ^{18}F-fluorodeoxyglucose; FOV = field of view; GGO = ground glass opacity; HRCT = high-resolution CT; HU = Hounsfield units; IRB = institutional review board; NSCLC = non-small cell lung cancer; OS = overall survival; RFS = recurrence-free survival; SUVmax = maximum standardized uptake value

Advances in radiologic techniques, such as high-resolution CT (HRCT) scanning and the widespread use of low-dose helical CT screening, have enabled frequent detection of early lung adenocarcinoma.[1-3] On HRCT scan, early lung adenocarcinoma often contains a nonsolid component, such as ground glass opacity (GGO), that is closely associated with a pathologic lepidic growth component.[4,5] Patients with GGO-dominant small lung adenocarcinoma are believed to have a good prognosis.[6] A recent study also demonstrated that patients with GGO-dominant clinical T1N0M0 lung adenocarcinoma (consolidation/tumor ratio ≤ 0.5 on thin-section CT scan) have an excellent prognosis after lobectomy.[7] Although patients with GGO-dominant tumors may be candidates for sublobar resection, there is no clear evidence to support this hypothesis.

For editorial comment see page 9

A prospective study that compared sublobar resection (wedge resection or segmentectomy) concomitant with lobectomy for clinical T1N0M0 non-small cell lung cancer (NSCLC) concluded that sublobar resection resulted in a high local recurrence and a low

survival rate.[8] However, sublobar resection for early lung cancer has been debated for a considerable amount of time. Several studies have demonstrated the usefulness of sublobar resection for peripheral small-sized NSCLC.[3,9-12] However, there currently is little evidence in patients who are optimal candidates for sublobar resection. Therefore, the present study aimed to characterize GGO-dominant clinical stage IA lung adenocarcinomas and to evaluate the prognosis of patients with these tumors after sublobar resection.

Materials and Methods

Patients

We evaluated the results of ^{18}F-fluorodeoxyglucose (FDG) PET/CT scans of 610 patients with clinical T1N0M0 stage IA lung adenocarcinoma from four institutions (Hiroshima University, Kanagawa Cancer Center, Cancer Institute Hospital, and Hyogo Cancer Center, Japan) between August 1, 2005, and June 30, 2010. Patients with incompletely resected tumors (R1 or R2) and those with multiple tumors or who had previously undergone lung surgeries were not included in our prospectively maintained database. Patient data obtained from this multicenter database were retrospectively analyzed for this study.

Patients underwent HRCT scanning and FDG-PET/CT scanning followed by curative R0 resection, and their tumors were staged according to the seventh edition of the *TNM Classification of Malignant Tumors*.[13] Mediastinoscopy or endobronchial ultrasonography was not routinely performed because all patients had undergone preoperative HRCT scanning and FDG-PET/CT scanning. HRCT scanning and FDG-PET/CT scanning revealed an absence of a >1 cm enlargement in mediastinal or hilar lymph nodes and an absence of >1.5 accumulation for the maximum standardized uptake value (SUVmax) in these lymph nodes, respectively. Sublobar resection was allowed in patients with complete disease removal as an optional procedure for a peripheral clinical T1N0M0 tumor that was intraoperatively assessed as N0 by frozen section evaluation of enlarged lymph nodes or by ensuring that there was no obvious enlargement of lymph nodes in the thoracic cavity. Systematic lymph node dissection, such as that of hilar and mediastinal nodes, was performed during segmentectomy but not during wedge resection. All patients showing pathologic lymph node metastasis received four cycles of platinum-based chemotherapy after surgery.

Manuscript received May 6, 2013; revision accepted July 12, 2013.
Affiliations: From the Department of Surgical Oncology (Drs Tsutani, Miyata, and Okada), Hiroshima University, Hiroshima; Department of Thoracic Surgery (Dr Nakayama), Kanagawa Cancer Center, Yokohama; Department of Thoracic Surgery (Dr Okumura), Cancer Institute Hospital, Tokyo; and Department of Radiology (Dr Adachi) and Department of Thoracic Surgery (Dr Yoshimura), Hyogo Cancer Center, Akashi, Japan.
Funding/Support: The authors have reported to *CHEST* that no funding was received for this study.
Correspondence to: Morihito Okada, MD, PhD, Department of Surgical Oncology, Research Institute for Radiation Biology and Medicine, Hiroshima University, 1-2-3-Kasumi, Minami-ku, Hiroshima City, Hiroshima 734-0037, Japan; e-mail: morihito@hiroshima-u.ac.jp

DOI: 10.1378/chest.13-1094

The inclusion criteria were preoperative staging determined through HRCT scan and FDG-PET/CT scan, curative surgery without neoadjuvant chemotherapy or radiotherapy, and a definitive histopathologic diagnosis of lung adenocarcinoma. This study was approved by the institutional review boards (IRBs) of the participating institutions (Hiroshima University Hospital IRB, No. EKI-644; Kanagawa Cancer Center IRB, No. KEN-31; Cancer Institute Hospital IRB, No. 2008-1018; Hyogo Cancer Center IRB, No. H20-RK-15). The requirement of informed consent from individual patients was waived because this study was a retrospective review of a patient database.

HRCT Scanning

Sixteen-row multidetector CT scanning was used to independently acquire chest images of subsequent FDG-PET/CT image examinations. The following parameters were used to acquire high-resolution tumor images: 120 kVp, 200 mA, 1- to 2-mm section thickness, 512×512-pixel resolution, 0.5- to 1.0-s scanning time, high-spatial reconstruction algorithm with a 20-cm field of view (FOV), and mediastinal (level, 40 Hounsfield units [HU]; width, 400 HU) and lung (level, -600 HU; width, 1,600 HU) window settings. GGO was defined as a misty increase in lung attenuation without obscuring the underlying vascular markings. A GGO-dominant tumor was defined as having a $>50\%$ GGO component. We defined a solid tumor size as the maximum dimension of the solid component measured on lung window settings, excluding GGO.[14] CT scans were reviewed and tumor sizes determined by radiologists from each institution.

FDG-PET/CT Scanning

Patients were instructed to fast for ≥ 4 h before IV injection of 74 to 370 MBq FDG and were subsequently advised to rest for ≥ 1 h before FDG-PET/CT scanning. Blood glucose levels were determined before tracer injection to confirm a <150 mg/dL level. Patients with blood glucose levels of ≥ 150 mg/dL were excluded from imaging. For imaging, a Discovery ST (GE Healthcare), an Aquiduo (Toshiba Medical Systems Corporation), or a Biograph Sensation 16 (Siemens AG) integrated three-dimensional PET/CT scanner was used. Low-dose, nonenhanced CT images of 2- to 4-mm section thickness for attenuation correction and localization of lesions identified with PET scan were acquired from head to pelvic floor in each patient by standard protocol.

Immediately after CT imaging, PET scanning was performed with an identical axial FOV for 2 to 4 min/table position, depending on condition of the patient and scanner performance. An iterative algorithm with CT scan-derived attenuation correction was used to reconstruct all PET images with a 50-cm FOV. We used an anthropomorphic body phantom (NEMA PET Sensitivity Phantom [NU2-2001]; Data Spectrum Corporation) to minimize variations in SUV among the institutions.[15] To decrease interinstitution SUV inconsistencies, a calibration factor was determined by dividing the actual SUV by the gauged mean SUV in the phantom background. The final SUV used in this study was referred to as the revised SUVmax.[16,17] The original SUVmax values were determined by radiologists from each institution.

Follow-up Evaluations

All patients who underwent lung resection were followed up from their day of surgery. For the first 2 years, postoperative follow-up procedures included a physical examination and chest roentgenogram every 3 months and chest and abdominal CT scan examinations every 6 months. Subsequently, a physical examination and chest roentgenogram were performed every 6 months, and a chest CT scan examination was performed each year.

Statistical Analysis

Results are presented as counts and percentages or as medians, unless stated otherwise. A χ^2 test was used to compare categorical variable frequencies. Fisher exact test was used when sample sizes were small. Recurrence-free survival (RFS) was defined as the time from the date of surgery until the first event (relapse or death from any cause) or the last follow-up. Overall survival (OS) was defined as the time from the date of surgery until death from any cause or the last follow-up. The Kaplan-Meier method was used to assess RFS and OS durations, and these were compared by log-rank test. To assess the potential independent effects of the surgical procedure on RFS, we used multivariate analyses with a Cox proportional hazards model. SPSS, version 10.5 (IBM Corporation) software was used for statistical analysis. The level of significance was set at $P < .05$.

Results

Table 1 shows the characteristics of patients with GGO-dominant tumors. Two hundred thirty-nine of 610 patients (39.2%) had GGO-dominant tumors that had a >50% GGO component. No 30-day postoperative mortality was observed for this population. The median follow-up period after surgery was 42.2 months. Patients with GGO-dominant tumors rarely had pathologically invasive tumors and lymph node metastases. Table 2 shows the distribution of operative procedures for each tumor size (clinical T1a and T1b). Sublobar resections, such as wedge resection and segmentectomy, were more likely performed in T1a tumors, whereas lobectomy was more likely performed in T1b tumors.

Recurrences developed in two patients with GGO-dominant tumors during the follow-up period (Table 3). One patient was an 82-year-old man with a 1.0-cm solid tumor size and with an SUVmax of 1.5 T1b (2.6 cm); peritoneal recurrence developed in this patient 23 months after left-sided S6 segmentectomy. The other patient was a 61-year-old woman with a 1.2-cm solid tumor size and a tumor SUVmax of 1.8 T1b (3.0 cm); brain metastasis developed in this patient 24 months after right-sided middle lobectomy.

Table 1—*Clinicopathologic Features of Patients With GGO-Dominant Tumors*

Variable	GGO-Dominant Tumors (n = 239)
Age, y	65 (31-89)
Male sex	94 (39.3)
Whole tumor size, cm	1.8 (0.7-3.0)
Solid tumor size, cm	0.2 (0-1.2)
SUVmax	0.9 (0-9.8)
Clinical T descriptor	
1a	155 (64.9)
1b	84 (35.1)
Procedure	
Lobectomy	90 (37.7)
Segmentectomy	56 (23.4)
Wedge resection	93 (38.9)
Positive invasion	
Lymphatic	3 (1.3)
Vascular	2 (0.8)
Pleural	1 (0.4)
Positive lymph node metastasis	2 (0.8)

Data are presented as median (range) or No. (%). GGO = ground glass opacity; SUVmax = maximum standardized uptake value.

Table 2—*Distribution of Operative Procedures in Patients With GGO-Dominant Clinical T1a and T1b Lung Adenocarcinoma*

Procedure	T1a Tumor (n = 155)	T1b Tumor (n = 84)	*P* Value
Wedge resection	79 (50.9)	14 (16.7)	...
Segmentectomy	37 (23.9)	19 (22.6)	<.001
Lobectomy	39 (25.2)	51 (60.7)	...

Data are presented as No. (%). See Table 1 legend for expansion of abbreviation.

There was no significant difference in 3-year RFS among patients with GGO-dominant tumors who underwent lobectomy (96.4%), segmentectomy (96.1%), and wedge resection (98.7%, $P = .44$) (Fig 1A). Three-year OS also was not significantly different among patients with GGO-dominant tumors who underwent lobectomy (97.6%), segmentectomy (98.2%), and wedge resection (98.7%, $P = .66$) (Fig 1B).

There was no difference in pathologic invasiveness, including lymphatic, vascular, or pleural, between patients with T1a GGO-dominant tumors and those with T1b tumors (Table 4). For patients with T1b GGO-dominant tumors, there was no significant difference in 3-year RFS among those who underwent lobectomy (93.7%), segmentectomy (92.9%), and wedge resection (100%, $P = .66$) (Fig 1C). Likewise, there was no difference in 3-year OS among patients with T1b GGO-dominant tumors who underwent lobectomy (95.9%), segmentectomy (100%), and wedge resection (100%, $P = .56$) (Fig 1D).

A multivariate Cox proportional hazards model for RFS included the preoperative variables of age, sex, clinical T descriptor, solid tumor size, SUVmax, and surgical procedure. However, none of these variables were independent prognostic factors (Table 5).

Discussion

The results of this study showed that patients with GGO-dominant clinical stage IA lung adenocarcinomas rarely had pathologically invasive tumors and had an excellent prognosis. These findings were consistent with previous reports showing that GGO-dominant lung adenocarcinoma had low malignant potential and good prognosis.[6,7] In addition, the current study showed that 3-year RFS and OS after sublobar resection were similar to those after lobectomy, without significant differences in GGO-dominant clinical stage IA lung adenocarcinoma.

Table 3—*Recurrences in Patients With GGO-Dominant Tumors*

Patient	Age, y	Sex	Whole Tumor Size, cm	Solid Tumor Size, cm	SUVmax	Procedure	ly	v	pl	n	Recurrence Site	Outcome
1	82	M	2.6	1.0	1.5	Segmentectomy	0	0	0	0	Peritoneum	25 mo, alive
2	61	F	3.0	1.2	1.8	Lobectomy	0	0	0	0	Brain	67 mo, alive

F = female; ly = lymphatic invasion; M = male; n = lymph node metastasis; pl = pleural invasion; v = vascular invasion. See Table 1 legend for expansion of other abbreviations.

Sublobar resection generally is indicated for a small lung cancer, such as those ≤ 2 cm.[3,18,19] However, in the current study, GGO-dominant T1b tumors rarely showed pathologic invasiveness or lymph node metastasis. Moreover, there were no differences in 3-year RFS and OS between patients with GGO-dominant

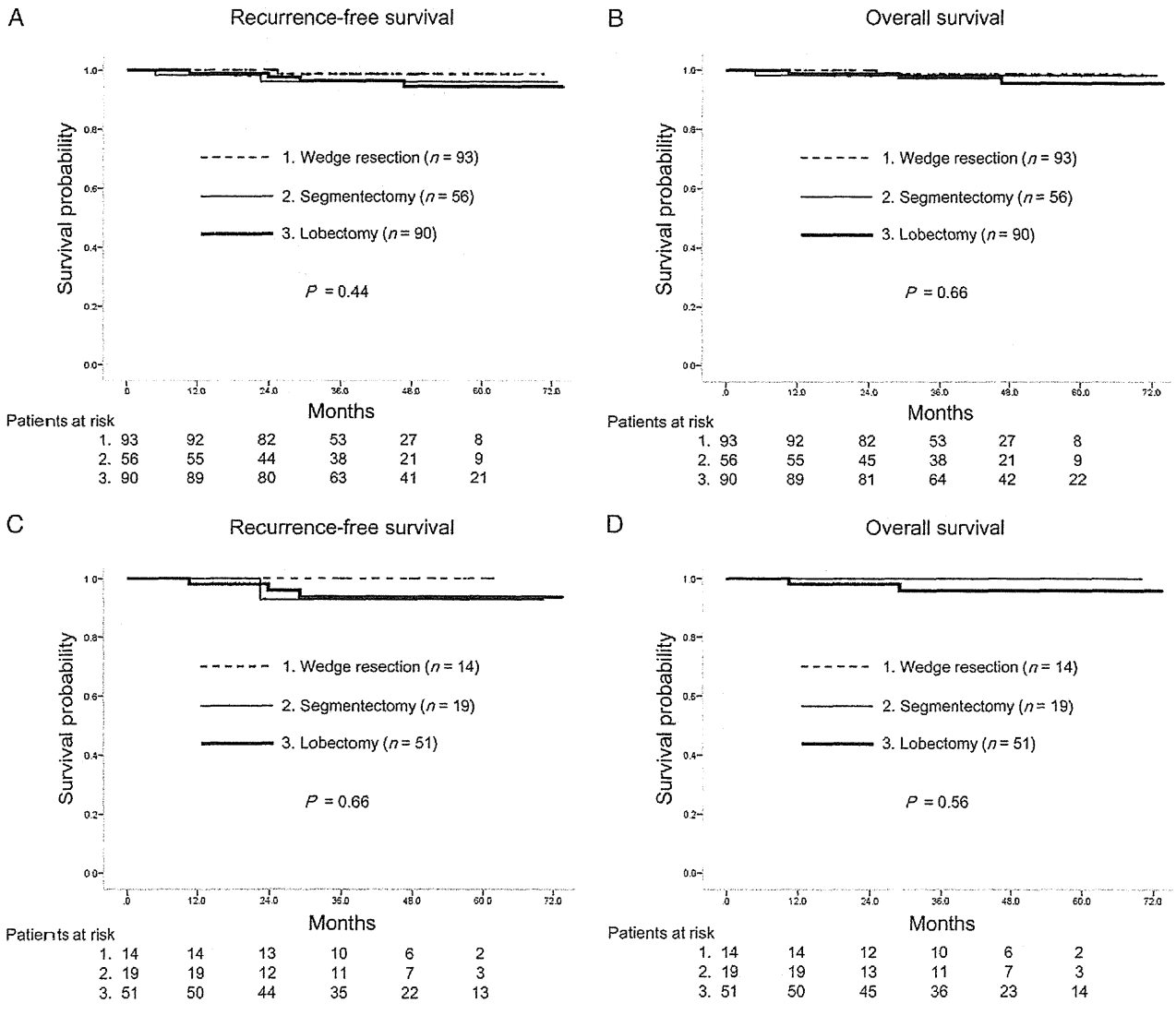

FIGURE 1. Recurrence-free survival (RFS) and overall survival (OS) curves for patients with ground-glass opacity (GGO) tumors who underwent lobectomy and sublobar resection. A, Three-year RFS rate for patients with GGO-dominant tumors who underwent wedge resection (98.7%; mean RFS, 69.8 mo; 95% CI, 68.6-70.9 mo), segmentectomy (96.1%; mean RFS, 70.3 mo; 95% CI, 67.3-73.4 mo), and lobectomy (96.4%; mean RFS, 71.4 mo; 95% CI, 61.9-73.7 mo; $P = .44$). B, Three-year OS rate for patients with GGO-dominant tumors who underwent wedge resection (98.7%; mean OS, 69.8 mo; 95% CI, 68.6-70.6 mo), segmentectomy (98.2%; mean OS, 71.4 mo; 95% CI, 69.0-73.7 mo), and lobectomy (97.6%; mean OS, 72.0 mo; 95% CI, 70.0-74.0 mo; $P = .66$). C, Three-year RFS rate for patients with GGO-dominant T1b tumors who underwent wedge resection (100%; mean RFS, not determined), segmentectomy (92.9%; mean RFS, 66.7 mo; 95% CI, 60.3-73.1 mo), and lobectomy (93.7%; mean RFS, 70.3 mo; 95% CI, 66.7-73.9 mo; $P = .66$). D, Three-year OS rate for patients with GGO-dominant T1b tumors who underwent wedge resection (100%; mean OS, not determined), segmentectomy (100%; mean OS, not determined), and lobectomy (95.9%; mean OS, 71.3 mo; 95% CI, 68.3-74.3 mo; $P = .56$).

Table 4—*Pathologic Findings for GGO-Dominant T1a and T1b Tumors*

Variable	T1a Tumors (n = 155)	T1b Tumors (n = 84)	*P* Value
Lymphatic invasion	1 (0.6)	2 (2.4)	.28
Vascular invasion	1 (0.6)	1 (1.2)	1.0
Pleural invasion	0 (0)	1 (1.2)	.35
Lymph node metastasis	0 (0)	2 (2.4)	.12

Data are presented as No. (%). See Table 1 legend for expansion of abbreviation.

T1b tumors who underwent lobectomy and those who underwent sublobar resection. Therefore, GGO-dominant T1b tumors could also be candidates for sublobar resection. We recommend segmentectomy and not wedge resection for sublobar resection of a GGO-dominant T1b tumor because these tumors could involve lymph node metastasis, and taking a sufficient surgical margin by wedge resection often is difficult in a T1b tumor.

In the current study, we found that two of 84 patients (2.4%) with GGO-dominant T1b tumors had lymph node metastases. No lymph node metastases were found for those with GGO-dominant T1a tumors. However, segmentectomy can approach hilar lymph nodes, whereas wedge resection cannot; thus, we should choose an optimal surgical procedure to avoid local recurrence in hilar lymph nodes, surgical stump, or residual lung. Segmentectomy would be superior to wedge resection for taking a sufficient surgical margin and for assessing hilar lymph nodes. Because sublobar resection includes both wedge resection and segmentectomy, it is necessary to distinguish between wedge resection and segmentectomy to clarify which procedure was used.

We encountered two distant recurrences with GGO-dominant T1b tumors: a brain metastasis after lobectomy and a peritoneal metastasis after segmentectomy, which could not be avoided even by standard lobectomy. One of the most important issues with sublobar resection is local control. Sublobar resection would be suitable for a GGO-dominant tumor because in this study, no intrathoracic local recurrence was observed, although a longer follow-up will be necessary before arriving at a definitive conclusion because of the indolent nature of GGO-dominant tumors.

Table 5—*Multivariate Analysis for Recurrence-Free Survival for Patients With GGO-Dominant Tumors*

Variable	HR (95% CI)	*P* Value
Age	1.08 (0.97-1.20)	.15
Male vs female sex	0.85 (0.18-3.91)	.83
T1b vs T1a descriptor	1.17 (0.20-6.70)	.86
Solid tumor size	6.37 (0.45-89.9)	.17
SUVmax	0.99 (0.52-1.90)	.99
Lobectomy vs sublobar resection	1.27 (0.20-7.93)	.82

HR = hazard ratio. See Table 1 legend for expansion of other abbreviations.

In the current study, the surgical procedure used and T descriptors were not independent prognostic factors of RFS in patients with GGO-dominant tumors, which also supports that a sublobar resection, such as a wedge resection or a segmentectomy, is suitable for GGO-dominant clinical stage IA lung adenocarcinomas, even for T1b tumors. In addition, solid tumor size and SUVmax were not independent prognostic factors of RFS. We previously reported that solid tumor size on HRCT scan and SUVmax on FDG-PET/CT scan were independent prognostic factors for lung adenocarcinoma.[14,20-22] However, patients with GGO-dominant lung adenocarcinomas have an excellent prognosis regardless of solid tumor size or SUVmax.

We speculate that GGO-dominant tumors indicate a uniform group exhibiting less tumor invasiveness and a favorable prognosis. In the current study, GGO-dominant tumors had small solid tumor sizes (median, 0.2 cm) and low SUVmax (median, 0.9). Prognosis based on solid tumor size and SUVmax may be useful, particularly for solid-dominant lung adenocarcinomas. In a previous study, we proposed N0 criteria that use a solid tumor size of < 0.8 cm or SUVmax of < 1.5 for predicting true N0 in clinical stage IA lung adenocarcinoma; patients who met these N0 criteria could be candidates for sublobar resection, such as wedge resection and segmentectomy.[11] Furthermore, patients with GGO-dominant tumors as well as those who meet the N0 criteria can be good candidates for wedge resection or segmentectomy.

Because this was a retrospective study, it is possible that patients who underwent sublobar resection were highly selective. Clinical trials comparing surgical results between lobectomy and sublobar resection (segmentectomy or wedge resection) for clinical T1aN0M0 NSCLC are currently being conducted by the Cancer and Leukemia Group B (CALGB 140503) and the Japan Clinical Oncology Group/West Japan Oncology Group (JCOG0802/WJOG4607L). These study results should indicate the significance of sublobar resection for small NSCLCs.[23] Regarding T1b tumors, a prospective study of segmentectomy for GGO-dominant tumors is warranted.

In conclusion, GGO-dominant clinical stage IA lung adenocarcinomas are a uniform group of tumors that exhibit low-grade malignancy and have a favorable prognosis. Patients with GGO-dominant tumors can be treated with wedge resection for T1a tumors and segmentectomy for T1b tumors.

ACKNOWLEDGMENTS

Author contributions: Drs Tsutani and Okada had full access to all the data in the study and take responsibility for the integrity of the data and the accuracy of the data analysis.

Dr Tsutani: contributed to study design, data acquisition, manuscript preparation, and approval of the final manuscript.
Dr Miyata: contributed to manuscript preparation and approval of the final manuscript.
Dr Nakayama: contributed to data acquisition, manuscript preparation, and approval of the final manuscript.
Dr Okumura: contributed to manuscript preparation and approval of the final manuscript.
Dr Adachi: contributed to manuscript preparation and approval of the final manuscript.
Dr Yoshimura: contributed to data acquisition, manuscript preparation, and approval of the final manuscript.
Dr Okada: contributed to study design, manuscript preparation, and approval of the final manuscript.
Financial/nonfinancial disclosures: The authors have reported to *CHEST* that no potential conflicts of interest exist with any companies/organizations whose products or services may be discussed in this article.

References

1. Aberle DR, Adams AM, Berg CD, et al; National Lung Screening Trial Research Team. Reduced lung-cancer mortality with low-dose computed tomographic screening. *N Engl J Med.* 2011;365(5):395-409.
2. Callol L, Roig F, Cuevas A, et al. Low-dose CT: a useful and accessible tool for the early diagnosis of lung cancer in selected populations. *Lung Cancer.* 2007;56(2):217-221.
3. Okada M, Koike T, Higashiyama M, Yamato Y, Kodama K, Tsubota N. Radical sublobar resection for small-sized non-small cell lung cancer: a multicenter study. *J Thorac Cardiovasc Surg.* 2006;132(4):769-775.
4. Nakata M, Saeki H, Takata I, et al. Focal ground-glass opacity detected by low-dose helical CT. *Chest.* 2002;121(5):1464-1467.
5. Jang HJ, Lee KS, Kwon OJ, Rhee CH, Shim YM, Han J. Bronchioloalveolar carcinoma: focal area of ground-glass attenuation at thin-section CT as an early sign. *Radiology.* 1996;199(2):485-488.
6. Kodama K, Higashiyama M, Yokouchi H, et al. Prognostic value of ground-glass opacity found in small lung adenocarcinoma on high-resolution CT scanning. *Lung Cancer.* 2001;33(1):17-25.
7. Asamura H, Hishida T, Suzuki K, et al; Japan Clinical Oncology Group Lung Cancer Surgical Study Group. Radiographically determined noninvasive adenocarcinoma of the lung: survival outcomes of Japan Clinical Oncology Group 0201. *J Thorac Cardiovasc Surg.* 2013;146(1):24-30.
8. Ginsberg RJ, Rubinstein LV; Lung Cancer Study Group. Randomized trial of lobectomy versus limited resection for T1 N0 non-small cell lung cancer. *Ann Thorac Surg.* 1995;60(3):615-622.
9. Jensik RJ, Faber LP, Milloy FJ, Monson DO. Segmental resection for lung cancer. A fifteen-year experience. *J Thorac Cardiovasc Surg.* 1973;66(4):563-572.
10. Nakayama H, Yamada K, Saito H, et al. Sublobar resection for patients with peripheral small adenocarcinomas of the lung: surgical outcome is associated with features on computed tomographic imaging. *Ann Thorac Surg.* 2007;84(5):1675-1679.
11. Tsutani Y, Miyata Y, Nakayama H, et al. Prediction of pathologic node-negative clinical stage IA lung adenocarcinoma for optimal candidates undergoing sublobar resection. *J Thorac Cardiovasc Surg.* 2012;144(6):1365-1371.
12. Tsutani Y, Miyata Y, Nakayama H, et al. Oncologic outcomes of segmentectomy compared with lobectomy for clinical stage IA lung adenocarcinoma: propensity score-matched analysis in a multicenter study. *J Thorac Cardiovasc Surg.* 2013;146(2):358-364.
13. Goldstraw P, Crowley J, Chansky K, et al; International Association for the Study of Lung Cancer International Staging Committee; Participating Institutions. The IASLC Lung Cancer Staging Project: proposals for the revision of the TNM stage groupings in the forthcoming (seventh) edition of the TNM Classification of Malignant Tumours. *J Thorac Oncol.* 2007;2(8):706-714.
14. Tsutani Y, Miyata Y, Nakayama H, et al. Prognostic significance of using solid versus whole tumor size on high-resolution computed tomography for predicting pathologic malignant grade of tumors in clinical stage IA lung adenocarcinoma: a multicenter study. *J Thorac Cardiovasc Surg.* 2012;143(3):607-612.
15. Mawlawi O, Podoloff DA, Kohlmyer S, et al; National Electrical Manufacturers Association. Performance characteristics of a newly developed PET/CT scanner using NEMA standards in 2D and 3D modes. *J Nucl Med.* 2004;45(10):1734-1742.
16. Nakayama H, Okumura S, Daisaki H, et al. Value of integrated positron emission tomography revised using a phantom study to evaluate malignancy grade of lung adenocarcinoma: a multicenter study. *Cancer.* 2010;116(13):3170-3177.
17. Okada M, Nakayama H, Okumura S, et al. Multicenter analysis of high-resolution computed tomography and positron emission tomography/computed tomography findings to choose therapeutic strategies for clinical stage IA lung adenocarcinoma. *J Thorac Cardiovasc Surg.* 2011;141(6):1384-1391.
18. Okada M, Yoshikawa K, Hatta T, Tsubota N. Is segmentectomy with lymph node assessment an alternative to lobectomy for non-small cell lung cancer of 2 cm or smaller? *Ann Thorac Surg.* 2001;71(3):956-960.
19. Yoshikawa K, Tsubota N, Kodama K, Ayabe H, Taki T, Mori T. Prospective study of extended segmentectomy for small lung tumors: the final report. *Ann Thorac Surg.* 2002;73(4):1055-1058.
20. Tsutani Y, Miyata Y, Yamanaka T, et al. Solid tumors versus mixed tumors with a ground-glass opacity component in patients with clinical stage IA lung adenocarcinoma: prognostic comparison using high-resolution computed tomography findings. *J Thorac Cardiovasc Surg.* 2013;146(1):17-23.
21. Tsutani Y, Miyata Y, Misumi K, et al. Difference in prognostic significance of maximum standardized uptake value on [^{18}F]-fluoro-2-deoxyglucose positron emission tomography between adenocarcinoma and squamous cell carcinoma of the lung. *Jpn J Clin Oncol.* 2011;41(7):890-896.
22. Tsutani Y, Miyata Y, Nakayama H, et al. Solid tumor size on high-resolution computed tomography and maximum standardized uptake on positron emission tomography for new clinical T descriptors with T1 lung adenocarcinoma. *Ann Oncol.* 2013;24(9):2376-2381.
23. Nakamura K, Saji H, Nakajima R, et al. A phase III randomized trial of lobectomy versus limited resection for small-sized peripheral non-small cell lung cancer (JCOG0802/WJOG4607L). *Jpn J Clin Oncol.* 2010;40(3):271-274.

厚生労働科学研究費補助金

がん臨床研究事業

切除可能悪性胸膜中皮腫に対する集学的治療法の確立に関する研究

平成２３年度～平成２５年度　総合研究報告書（Ⅱ）

研究代表者　中野 孝司

平成２６（２０１４）年　３月

厚生労働科学研究費補助金

がん臨床研究事業

切除可能悪性胸膜中皮腫に対する集学的治療法の確立に関する研究

平成２３年度～２５年度　総合研究報告書（Ⅱ）

研究代表者　中野　孝司

平成２６（２０１４）年　３月

総合研究報告(Ⅱ)目次

目　　次

Ⅳ. 研究成果の刊行物・別刷（Ⅱ）邦文

7．胸膜中皮腫（メソテリオーマ）

胸膜中皮腫とは

胸膜中皮腫とは，胸腔の内面と肺の表面を覆う胸膜の中皮細胞に発生する悪性腫瘍です。中皮細胞が断熱材などに使われてきたアスベストを吸ったことが原因でがん化します。アスベストを吸ってから中皮腫ができるまでは，約 40 年かかります。胸膜のあらゆる所に広がるので「びまん性悪性胸膜中皮腫」とも言います。アスベスト関連の職歴がある場合は労災に，ない場合は石綿健康被害救済法の公的補助の対象になる悪性腫瘍です。生活環境も発症に関係しますので，患者さんと同じ環境にいた方は念のために検診を受けることをお勧めします。

検査・診断の方法

中皮腫は，肺がんとは異なる部位に発生します。ほとんどの胸膜中皮腫は胸水貯留がみられますので，まず胸水を調べます。中皮腫を疑う悪性細胞が得られていても胸膜生検は必要です。細胞診だけでは中皮腫の確定診断ができないからです。

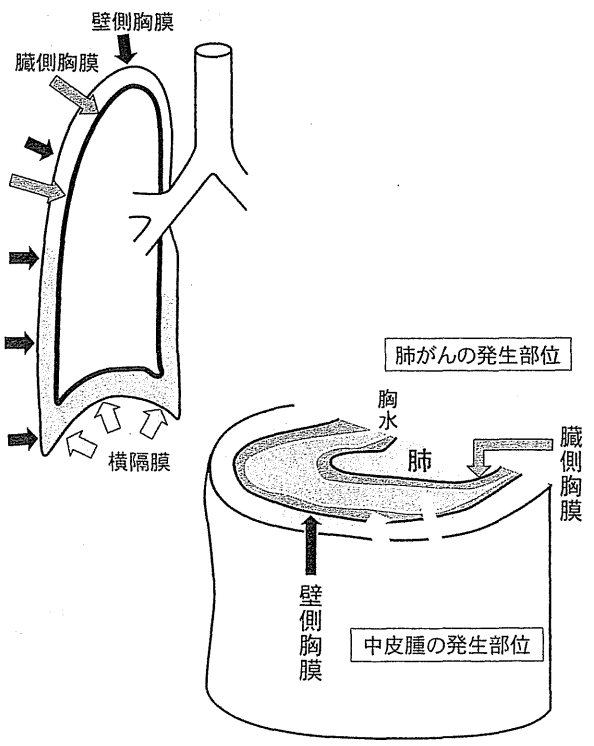

壁側胸膜・臓側胸膜・肺の位置関係

生検で確実な方法は胸腔鏡検査です。早期の中皮腫では，臨床病期の決定に必要な検査です。また，アスベスト曝露のある原因不明の胸水には実施すべき検査です。

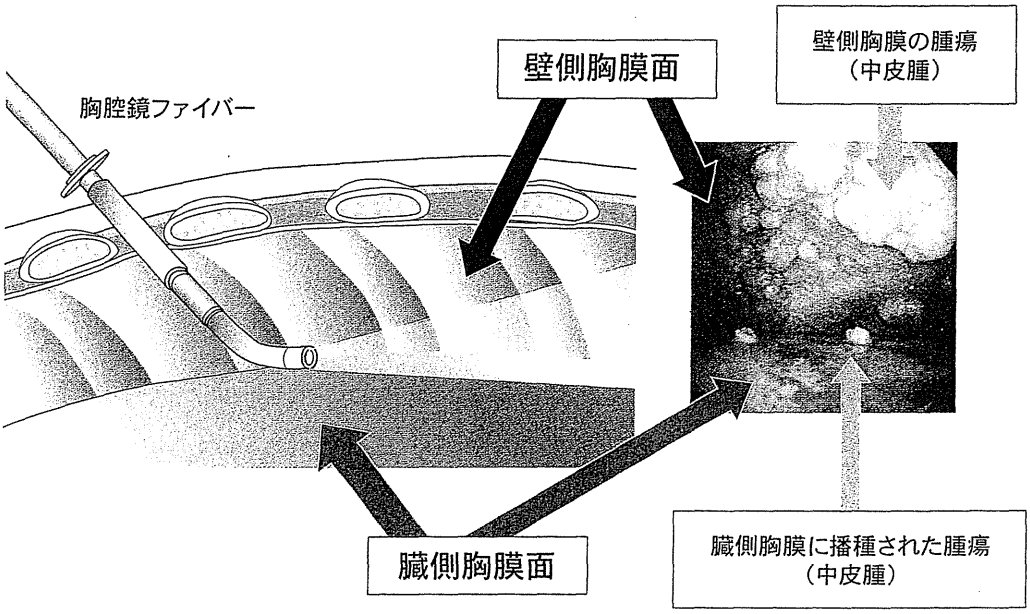

胸腔鏡による胸腔内の観察
胸膜中皮腫の胸腔内所見（臨床病期 T1b 期）。

中皮腫の種類

中皮腫は病理組織所見で，上皮型，肉腫型，および両者が混在する二相型の３亜型に分類します。組織亜型により，治療の効果，予後がかなり異なります。上皮型は抗がん剤治療の成績が期待できるのですが，肉腫型はほとんど効果がありません。

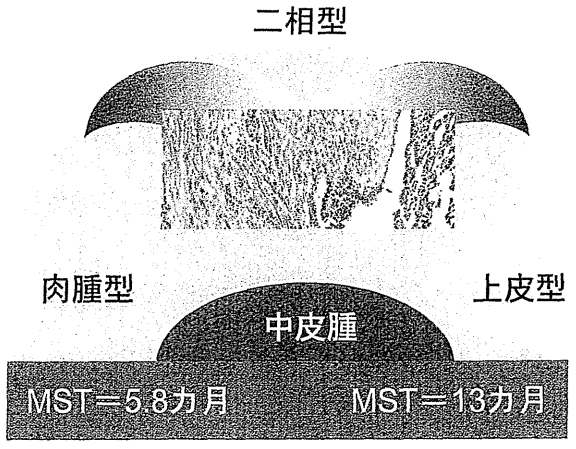

中皮腫の組織亜型
MST：median survival time；生存期間中央値

初発からの発育経過と臨床症状

最も早期には中皮腫は壁側胸膜に限局し，臓側胸膜に腫瘍はみられません。この時期をT1a期と言います。次に，臓側胸膜に腫瘍が播種されます。この時期がT1b期です。T1期は，腫瘍は小さく，主に胸水による症状がみられます。縦隔を変位させる程の胸水が溜まることもあります。その後，すべての胸膜面に急速に広がり（T2期），典型的なCT所見がみられるようになります。周囲への浸潤が高度となり，横隔膜を越えて腹腔に達すると腹水が，心膜に浸潤すると心嚢液が貯留します。

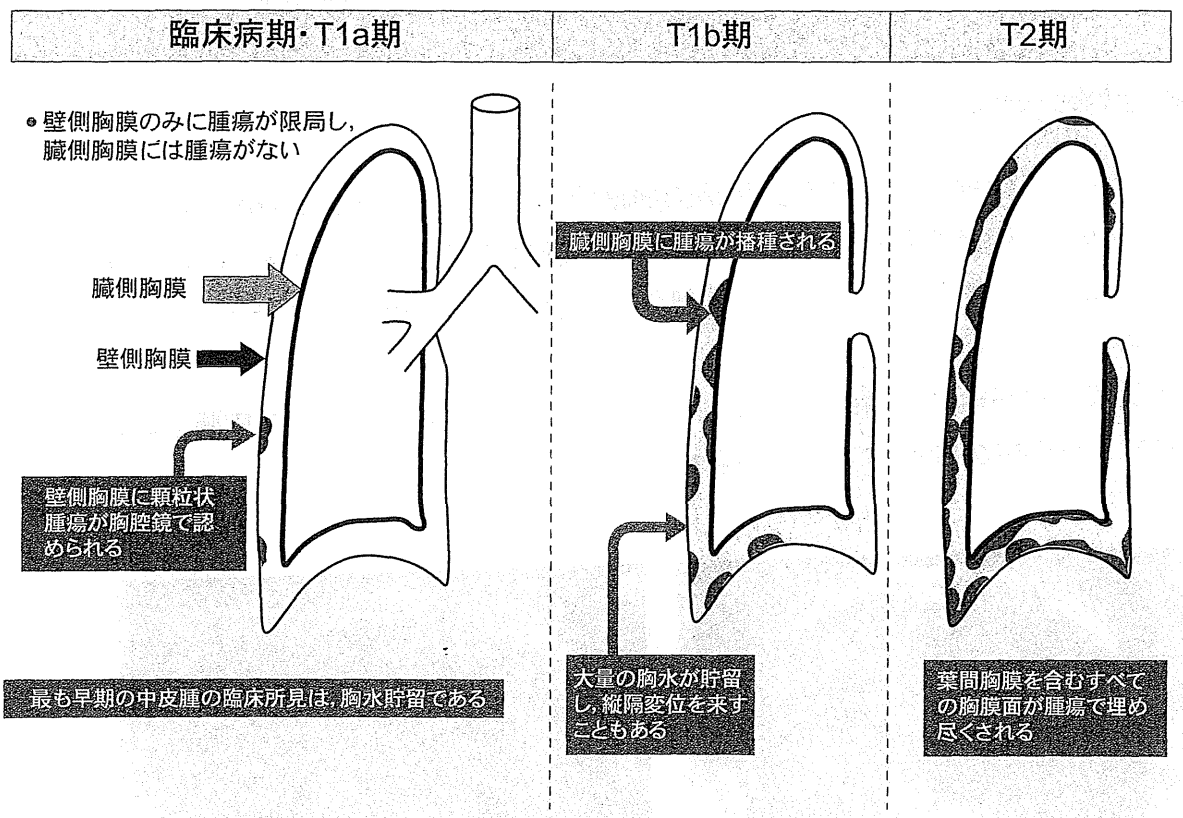

胸膜中皮腫の初発からの発育経過

化学療法

胸痛などの症状があれば，まずその症状を緩和させる治療を行います。全身状態が良好で，抗がん剤治療が可能な場合はシスプラチン（またはカルボプラチン）とペメトレキセドによる化学療法を行います。この治療法は，シスプラチンだけの治療よりも生存期間が延びることが証明されています。

外科治療

肺を残すようにして腫瘍をできる限り切除する胸膜切除 / 肺剥皮術と，胸膜・肺・横隔膜・心膜を塊として大きく切除する胸膜肺全摘術があります。前者は，わが国ではほとんど行われていません。後者を早期例に行い，腫瘍を全部取り切っても，顕微鏡的にがん細胞が残ります。中皮腫が胸膜にできるので切除マージンがとれないからです。術後，高率に再発しますので，抗がん剤治療と術後の放射線治療の併用が必要です。

この胸膜肺全摘術には５～９％の手術関連死亡率があります。上皮型，女性，良好な全身状態，胸痛がない，血小板増多がない，などの良い条件が揃うと治療の良い面が出てきますが，予後不良因子が多い場合は，この治療法は勧められません。

放射線治療

放射線治療は，疼痛緩和，胸腔穿刺路の腫瘍播種予防，術後の再発予防の目的で行われます。中皮腫は胸腔穿刺路やドレーン挿入部に腫瘍播種が起こりやすいので，予防照射が行われることがあります。しかし，無作為化比較試験で有効性が示されなかったので，最近はほとんど行われていません。

強度変調放射線治療は，複雑な形状に合わせた照射が可能ですので中皮腫に応用されていますが，有効性の評価はできていません。

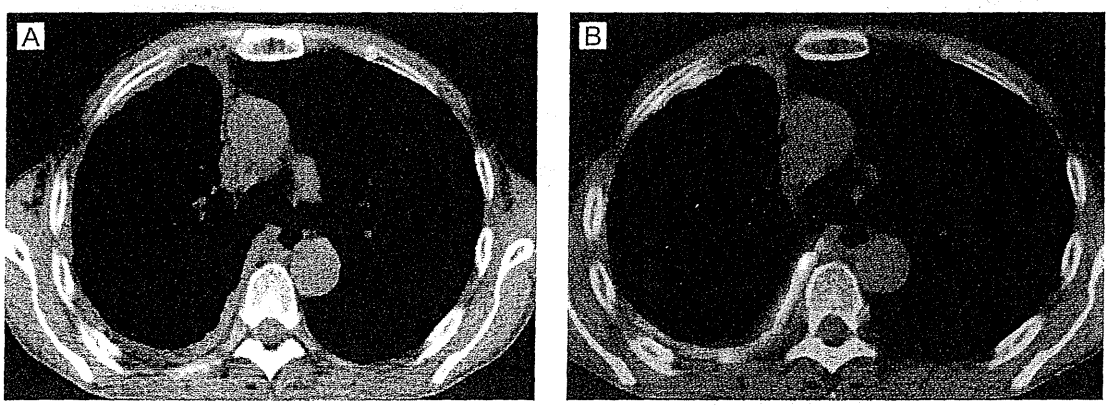

すべての胸膜が腫瘍化した典型的な悪性胸膜中皮腫（T2 期）

A：CT 像
B：FDG-PET 像

（中野 孝司）